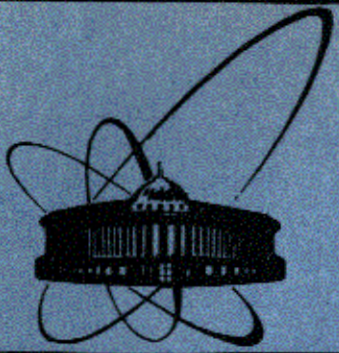

объединенный
институт
ядерных
исследований
дубна

E14-84-339

E.Kuzmann, I.N.Spirov

MÖSSBAUER STUDY OF AMORPHOUS ALLOYS IRRADIATED WITH ENERGETIC HEAVY IONS

Submitted to "Journal of Nuclear Materials"

1984

1. INTRODUCTION

In the last ten years investigations of radiation damages in amorphous materials receive considerable attention since these materials can provide information on their structure and structural changes and can be used as the first wall of a thermonuclear reactor.

Investigations have already been carried out on metal-metal and metal-metalloid amorphous systems (being in different states) irradiated with electrons, neutrons, protons, light and heavy ions (having different energies and doses) by applying a lot of methods, such as X-ray and electron diffraction, calorimetry, electron microscopy, dilatometry, electrical resistivity and positron annihilation, as density measurements[1-26].

The materials and methods used, and the results and conclusions of some representative studies are summarised in Table I.

It is very difficult to compare the results of different investigations, first of all, because of differences in the states of the investigated systems, as well as in the interactions due to the various irradiations.

It is shown that the amorphous alloys, compared with crystalline ones, have very high resistance to radiation damage. However the significant changes in some physical properties caused by irradiation demonstrate that metallic glasses can be structurally modified by irradiation.

The Mössbauer spectroscopy is a useful tool for the investigation of amorphous alloys because the interactions (electrical monopole and quadrupole, magnetic dipole) measured by this method offer a unique possibility of providing information about the surrounding of a Mössbauer atom[27]. It was already applied successfully many times to study magnetic and structural properties as well as the crystallisation process in amorphous metals (see, e.g., refs.[28-31]).

During the last year some attempts were made to use the Mössbauer spectroscopy for studying radiation effects in amorphous materials, too[13,18,25].

The aim of the present work was to obtain information about radiation damages in metal-metalloid amorphous alloys irradiated with energetic heavy ions with the help of Mössbauer spectroscopy.

Table I

Materials and methods used, results and conclusions of some representative studies of radiation effect in amorphous materials

Author	Material	Irradiation	Methods	Results	Conclusions
Leseueur /1/	$Pd_{80}Si_{20}$	Fission fragment 10^{13} -10^{14} ff/cm²	electrical resistivity	R/R_0 increases with increasing dose up to 10^{13} ff/cm²	Induced amorphous state by atomic collisions is different from obtained by splat cooling in local ordering of atoms
Nanao et al. /2/	$Fe_{80}B_{20}$, $Pd_{80}B_{20}$	electron E = 1.25 MeV up to 10^{22} e/cm²	TEM, SEM	No changes	High resistance to radiation damages
Hautojärvi et al. /3,4/	$Fe_{40}Ni_{40}P_{14}B_6$ $Fe_{80}B_{20}$, $Pd_{80}Si_{20}$	electron E = 3 MeV up to $3 \cdot 10^{19}$ e/cm²	positron annihilation	The positron lifetime increases, depending on the material; heat treatment can restore the initial lifetime	High resistance to radiation damages; recovery of irradiation induced defects occurs smoothly over a wide temperature range
Hillairet et al. /20/	$Fe_{50}Ti_{50}$, $Ni_{40}Nb_{60}$ $Cu_{40}Zr_{60}$	electron E = 2.5 MeV up to 10^{18} e/cm²	electrical resistivity	R/R_0 increases after irradiation, defects created are annealed over the entire temperature range	Defects created by irradiation undergo only a small number of diffusional pumps before getting eliminated which restrict their contribution to ordering
Nandedkar et al. /5/	$Ni_{45}Fe_5Co_{20}Cr_{10}Mo_4B_{16}$	electron from accelerator $4 \cdot 10^{16}$ e/cm² from HVEM 10^{21} e/cm²	Hot stage TEM X-ray diffr. DSC, el.resist.	No noticeable changes	No noticeable change in the onset of crystallisation for electron irradiation
Kramer et al. /6/	$/Mo_{0.6}Ru_{0.4}/_{82}B_{18}$	neutron 10^{19} n/cm² 0.1-1 dpa	X-ray diffr. density, el. resistivity, ductility, temp. of superconducting transition	1.5% decrease of density; 70% decrease of width of superconducting transition; 7% increase of width of the main peak of X-ray diffr.; ductility improves	Irradiation induced defects have atomic scale dimensions and lead to excess free volume
Itoh et al. /7/	$Mo_{62}Si_{32}$	neutron $9 \cdot 10^{18}$ n/cm² E > 1 MeV	positron ann. X-ray diffr. el. resistivity	Small increase in positron lifetime; height of first and second peaks in S/Q/ are slightly lowered; superconducing transition becames sharp	Degree of disorder of structure increases; cluster of vacancies can not be introduced
Doi et al. /8,9/	$Pd_{80}Si_{20}$	neutron $5 \cdot 10^{20}$ n/cm² E > 1 MeV	X-ray diffract.	Changes in small angle region of diffraction pattern	Coherent regions (of 8 Å diameter) get separated from each other by a mean distance of 20 Å due to irradiation
Gerling and Wagner /10/	$Fe_{40}Ni_{40}B_{20}$	neutron up to $6.5 \cdot 10^{19}$ n/cm² (thermal and fast neutrons)	DSC, TEM bending test	Decrease of crystallisation temperature; dpa dependent increase of Curie temperature; bubble-like structure in TEM; loss in ductility	No crystallisation due to irradiation; embrittlement occurs without devitrification
Cahn et al. /11/	$Ni_{64}Zr_{36}$ $Ni_{33}Zr_{67}$ (annealed)	neutron E > 1 MeV up to $1.1 \cdot 10^{20}$ n/cm²	DSC, X-ray diff., dilatometry, diffusivity	Changes in comparative DSC plots according to a preliminary heat release; diffusion of gold is an order of magnitude slower; differences in the crystallisation processes	Changes in short range order due to irradiation; polymorphously formed microcrystals during the preliminary heat release

Cline et al. /12/	$Fe_{40}Ni_{40}P_{14}B_6$ (annealed)	neutron E > 0.1? MeV $1.2 \cdot 10^{19}$ E > 0.92 MeV $4.5 \cdot 10^{18}$ n/cm²	DSC X-ray diffr. bending test
Goldanskii et al. /13/	$Co_{83}Fe_{6.5}Si_{8.5}B_2$	neutron (thermal) 10^7 n/s·cm²	Mössbauer spectroscopy "in situ"
Yadawa et al. /14/	$Fe_{40}Ni_{40}P_{14}B_6$	proton E = 250 keV up to 10^{19} p/cm²	SEM
Tyagi et al. /15/	$Fe_{40}Ni_{38}Mo_4B_{18}$ $Fe_{40}Ni_{40}B_6P_{14}$	He ion E = 50 keV up to $3 \cdot 10^{18}$ ion/cm²	SEM, TEM
Pászti et al. /16,17/	$Fe_{32}Ni_{36}Cr_{14}P_{12}B_6$ and others	He ion E = 1-2 MeV 10^{18} ion/cm²	SEM, TEM
Nasu and Fujita /18/	$Fe_{82.3}Si_9B_{8.5}$	He ion E = 100 keV 10^{16} - 10^{18} ion/cm²	Conversion electron Mössbauer spectroscopy
Van Swijgenhoven and Stals /19/	$Fe_{40}Ni_{38}Mo_4B_{18}$	Ar ion E = 5 keV $5 \cdot 10^{17}$ ion/cm²	TEM, SEM
Chang and Li /24/	$Fe_{40}Ni_{40}P_{16}B_6$	Ni ion E = 60 MeV up to 86 dpa	Profilometry (swelling)
Rechtin et al. /22/	$Nb_{40}Ni_{60}$	Ni ion E = 5 MeV up to 20 dpa	TEM
Brimhall et al. /23/	Mo-Ni	Ni ion E = 5 MeV up to 86 dpa	TEM
Azam et al. /21/	Ni ion E = =500 keV up to 100 dpa	Ni ion E = 500 keV up to 100 dpa	TEM
Kurmann and Spirov /25/	$Fe_{10}Ni_{70}P_{20}$ $Fe_8/Co, Cr, Ni, Mn/B_{15}Si_8$ $Fe_{40}Ni_{40}B_{10}Si_{10}$	Ar ion E = 225 MeV Xe ion E = 120 MeV	Mössbauer spectroscopy
Audoard et al. /26/	$Fe_{80}B_{20}$ $Fe_{78}Mo_2B_{20}$	electron E = 25 MeV fast neutron fission fragment	electrical resistivity

The ductility improves due to irradiation; peak of apparent heat capacity of the so received material disappears completely	The irradiation destroys the original phase separation; defects are induced
Phases of Fe/Co/ and Fe_3B appear in Mössbauer spectra recorded after $^{56}Fe/n, \gamma/^{57}Fe$ nuclear reaction in situ using the target as an emitter	Crystallisation caused by nuclear reactions
No blistering in irradiated amorphous materials	High resistance to radiation damage
Blistering at critical dose, which increases with increasing beam energy; gas bubble formation from 10^{17} ion/cm²	Partial crystallisation associated with gas bubble formation
Flacking; pattern formation on the surface remaining behind the flacked layer; edge dislocationlike imperfections	Pattern formation is connected with the migration of the ion and its accumulation into gas bubbles
Emergence of α-iron component in CEMS spectra at dose higher than 10^{18} ion/cm²	Partial crystallisation on the surface
Amorphous layer (~ 7 nm) formation on recrystallized material; blistering	Amorphisation on recrystallized materials
Dose dependent swelling in irradiated samples	Existence of regions of positive excess volume
No changes are in amorphous state, but irradiation with 1 dpa is enough for complete amorphisation of crystalline	High resistance to radiation damage; defects are possible as very small clusters or atomic vacancies due to irrad.
No changes are at low temperature; irradiation at 857 K produces crystallisation in amorphous but do not produce amorphisation in crystalline	Irradiation at elevated temperature accelerates the thermally activated processes
No change due to irradiation at room temperature; irradiation at 200°C lowers the crystallization temperature	Differences between the amorphous states at different temperatures
Decrease of the intensity of 2nd and 5th lines of Mössbauer spectra in according to decrease of magnetic anisotropy	Defects created by irradiation; processes due to irradiation are opposite to that of low temperature relaxation
Electrical resistivity increases with increasing dose, than it shows a saturation effect	Creation point defects in the short range order and induced structural changes due to irradiation

2. EXPERIMENTAL

Amorphous alloys $Fe_{40}Ni_{40}B_{20-x}Si_x$, $(0 \leq x \leq 10)$ and $Fe_xNi_{80-x}P_{20}$, $(5 \leq x \leq 20)$, in the form of a continuous, rapidly quenched ribbon about 25 μm thick, were investigated.

Samples of the above-mentioned alloys were placed onto a Cu target backing by sticking with a special silver glue. Some samples of all compositions were covered by thin Cu foils (the thickness of which was a little bit larger than the penetration depth of radiation). These samples served for the control of irradiation.

The irradiation of samples was carried out at room temperature with ^{40}Ar (E = 225 MeV) or ^{132}Xe (E = 120 MeV) ions with doses 10^{13} - 10^{14} ions/cm^2 at the U-300 cyclotron of the Laboratory of Nuclear Reactions of the JINR. The ion beam was scanned on the whole target in order to achieve homogeneous irradiation. The different doses were obtained by screening different parts of the target. There was no elevation of temperature on the target backing measured by a thermocouple.

The displacement per atom was estimated very roughly by calculations [35] to be 0.2-2 dpa and up to 5 dpa at peak for Ar and Xe irradiation, respectively.

The Mössbauer spectra of nonirradiated, irradiated and control samples were recorded with two conventional constant acceleration Mössbauer spectrometers with an asymmetrical triangular drive using 512 channels. The Mössbauer measurements were carried out at room temperature and at the temperature of liquid nitrogen. The spectra were obtained in transmission geometry and sometimes in reflection geometry. The same CEMS detector was used as previously [32]. 67 mCi and 30 mCi activity ^{57}Co sources in Rh matrix, kept at room temperature, provided γ-rays. The velocity calibration was made using a 7 μm very pure α-Fe foil.

The evaluation of all Mössbauer spectra was carried out by least-squares fitting of Lorentzians. In the case of ferromagnetically splitted spectra the magnetic hyperfine field distribution was also obtained by Fourier analysis with the same program, as used in [33]. These calculations were perfromed at the CDC-6500 computer of the JINR.

3. RESULTS

Figure 1 shows the transmission Mössbauer spectra, recorded at room temperature, of $Fe_{40}Ni_{40}B_{10}Si_{10}$ amorphous samples (nonirradiated, control) with shielding on the target backing (and irradiated with 225 MeV ^{40}Ar ions with different doses), as representative ones. The spectra, which are typical for ferromagnetic metallic glasses, exhibit magnetically splitted patterns with six broad absorption lines. They can be considered as superpositions of a variety of spectra belonging to iron atoms having different neighbourhood. Hence a distribution in hyperfine parameters occurs, namely in the magnetic hyperfine field, H isomer shift, δ, and quadrupole splitting ΔE_Q. The average hyperfine parameters of spectra were determined by least-squares fitting of lines, as in [34]. The Mössbauer parameters obtained by least-squares fitting served as input parameters for the evaluation of the hyperfine field distribution by Fourier transformation.

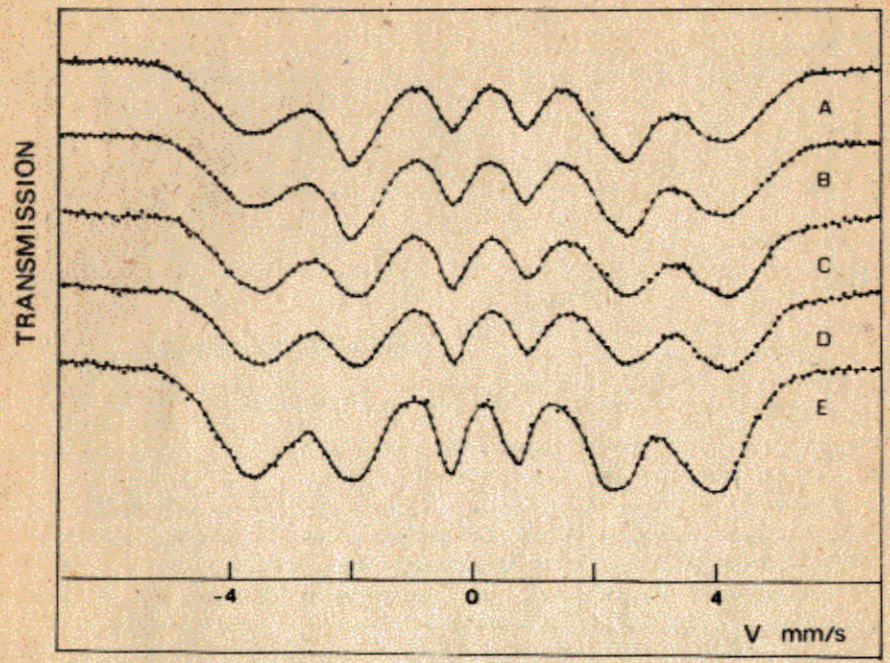

Fig. 1. Mössbauer spectra, recorded at room temperature, of $Fe_{40}Ni_{40}B_{10}Si_{10}$ amorphous alloys A) nonirradiated, B) control: being with shielding on the target backing, C)-E) irradiated with ^{40}Ar ions (E = 225 MeV) with 10^{13}, $3 \cdot 10^{13}$ and 10^{14} ion/cm^2 doses, respectively.

No changes were observed in the Mössbauer spectra of control samples compared to that of nonirradiated ones, in any case. This means that the changes in the spectra of the irradiated sample are due to irradiation.

The spectra of the irradiated amorphous samples exhibit the following changes.

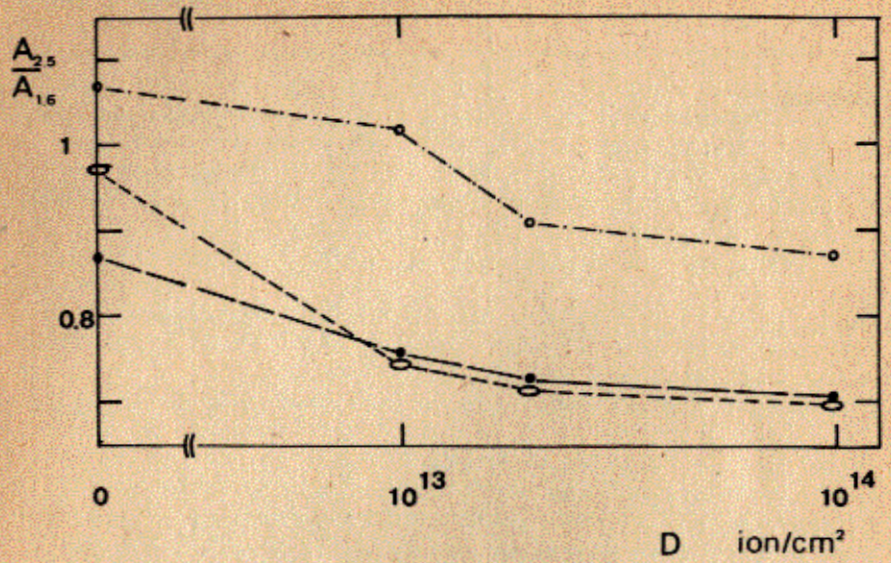

Fig.2. Dose dependence of relative areas of absorption lines ($A_{2.5}$ and $A_{1.6}$) of Mössbauer spectra of some Ar-irradiated $Fe_{40}Ni_{40}B_{20-x}Si_x$ amorphous alloys (o x = 0, x = 5, • x = 10).

The main difference between the spectra of nonirradiated and irradiated samples were observed in the change of intensity of the 2nd and 5th lines, as can be seen in Fig.1. From the comparison of spectra of irradiated samples (Fig.1C-E) with that of nonirradiated or control samples (Fig.1A, B) not only the decrease of the intensity of these lines, but its dose dependence is also visible. Such a dose dependence of the relative areas of absorption lines ($A_{2,5}$ and $A_{1.6}$) are plotted in Fig.2 in the case of some Ar-irradiated $Fe_{40}Ni_{40}B_{20-x}Si_x$ amorphous alloys.

Similar changes may be observed in the case of ^{132}Xe ion irradiation. These are represented in Fig.3, where the Mössbauer spectra of amorphous samples (Fig. 3A nonirradiated and Fig.3B irradiated with fluence $5 \cdot 10^{13}$ ion/cm^2) are shown.

Dose dependent changes of the evaluated Mössbauer parameters were also found. The average hyperfine field decreases with increasing doses, as illustrated in a representative case in Table II. The average isomer shift changes within the experimental error.

There are dose dependent differences between the hyperfine field distributions of the nonirradiated and the irradiated samples. For illustration the hyperfine field distributions of the nonirradiated and Ar-irradiated amorphous alloys are shown

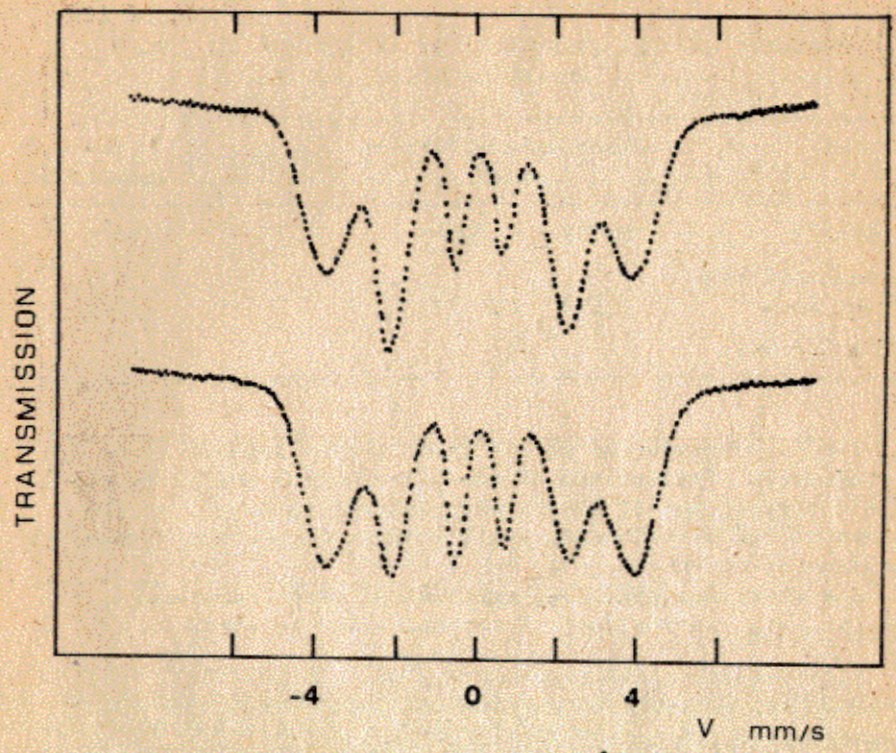

Fig.3. Mössbauer spectra, recorded at room temperature, of amprphous alloy A (nonirradiated, B) irradiated with ^{132}Xe ions (E = 120 MeV) with a fluence of $5 \cdot 10^{13}$ ion/cm^2.

Table II

Measured average hyperfine fields of $Fe_{40}Ni_{40}B_{10}Si_{10}$ amorphous alloys

State	Hyperfine field (MA(m)	Meas. Temperature
Initial	19.173±0.035	room
Irradiated with ^{40}Ar ions		
10^{13} ion/cm^2	19.058±0.037	room
$3 \cdot 10^{13}$ ion/cm^2	19.039±0.035	room
10^{14} ion/cm^2	18.980±0.035	room

Table III

Measured average quadrupole splittings of $Fe_{10}Ni_{70}P_{20}$ amorphous alloy

State	Quadrupole splitting /mm/s/	Meas. Temperature
Initial	0.559 ± 0.0034	room
Irradiated with ^{40}Ar ions /E = 225 MeV/	0.542 ± 0.0029	room

in Fig.4. A broadening of the distribution appears to be due to irradiation. The maximum of the distribution shifts to the low field region, and it lowers with increasing doses. In the shape of the distribution small changes can be seen around the maximum.

The Mössbauer spectrum, recorded at room temperature, of $Fe_{10}Ni_{70}P_{20}$ paramagnetic amorphous alloy is shown in Fig. 5.

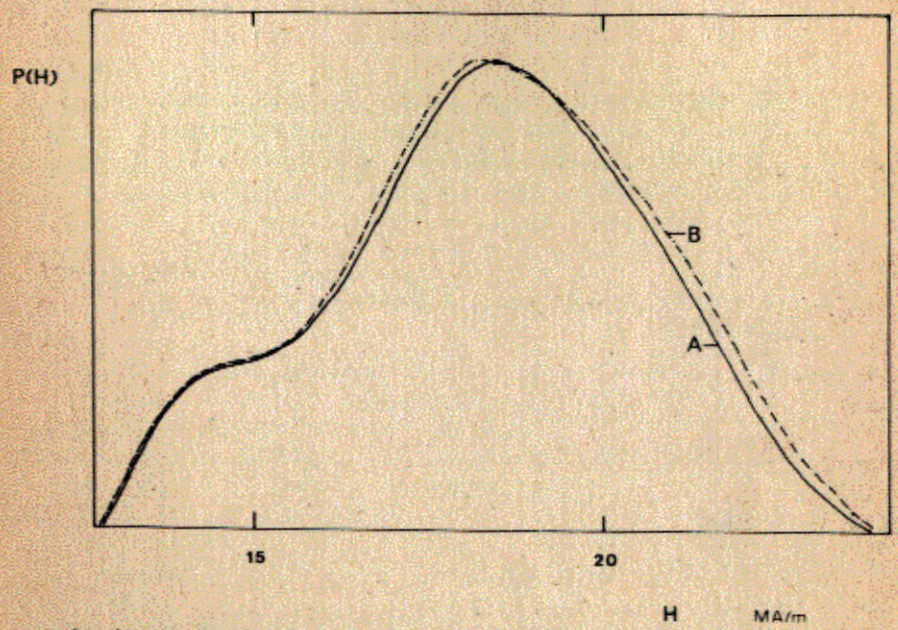

Fig.4. Hyperfine magnetic field distribution of $Fe_{40}Ni_{40}B_{15}Si_5$ amorphous alloys A) nonirradiated, B) irradiated with ^{40}Ar ions (E=225 MeV).

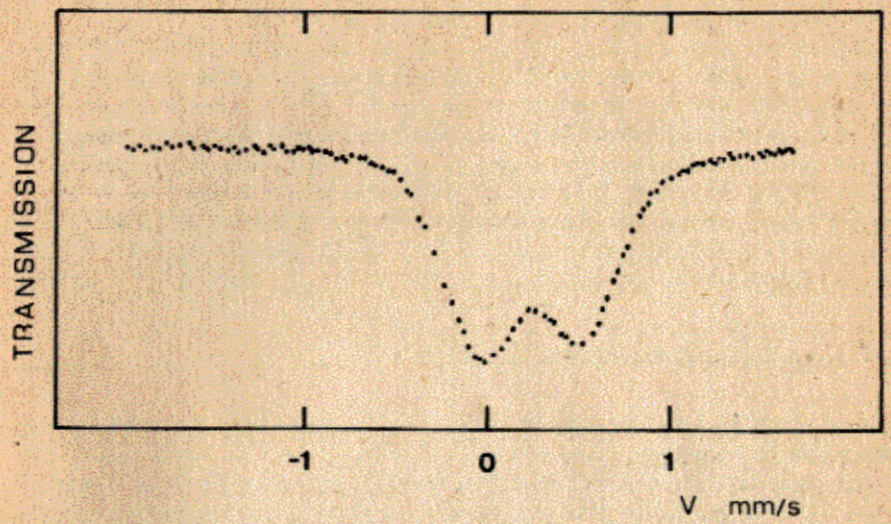

Fig.5. Mössbauer spectrum of $Fe_{10}Ni_{70}P_{20}$ paramagnetic amorphous alloy, recorded at room temperature.

The spectrum consists of slightly asymmetrical pairs of lines corresponding to a paramagnetic amorphous state. The evaluated average quadrupole splitting slightly decreases due to irradiation, as can be seen in Table III.

4. DISCUSSION

First of all the results together with other Mössbauer results [13, 18, 25] indicate the applicability of Mössbauer spectroscopy as a promising method for investigation of radiation effects in amorphous alloys.

Our results cannot be compared with the result of the cited investigations [13, 18] because of the fundamental difference between the groups of atoms observed using different measurements techniques. In the work of Nasu and Fujita [18] and Goldanskii et al. [13] radiation effects were found only in a very thin surface layer or in iron atoms involved in nuclear reactions by monitoring them with special, selectively sensitive Mössbauer techniques. In our case the Mössbauer spectra were recorded in transmission geometry, providing integral information about the iron atoms (and its surroundings) being in the whole sample, the thickness (25 μm) of which was slightly larger than the penetration depth of energetic heavy ions (23 μm for ^{40}Ar) used for irradiation. Consequently we cannot distringuish between the effect of electron excitation (thermal spike) and

an atomic collision (cascades), which are the main interactions in the case of energetic heavy ion irradiation.

However, by analysing our spectra we can obtain some information, e.g., about the magnetic anisotropy [28], the topological and chemical short-range order (e.g., [29,30]), which determine the fundamental physical properties of amorphous materials.

The observed intensity changes of the 2nd and 5th lines of Mössbauer spectra (Fig.2) of ferromagnetic amorphous alloys due to irradiation are connected with the changes of the average direction of magnetic moment [41], which were determined from the relative areas of absorption lines ($A_{2.5}$ and $A_{1.6}$) by the formula

$$A_{2.5} / A_{1.6} = 4 \sin^2 \theta / 3 (1 + \cos^2 \theta), \qquad (1)$$

where θ is the angle between the γ ray direction and the average direction of magnetic moment.

The results obtained from the data presented in Fig.2 are shown in Fig.6. They give information about the magnetic anisotropy due to the distribution of spin direction (domen structure) or preferred spin orientation (spin texture), in these materials.

The γ ray direction, which was parallel to that of the incident ion beam, was perpendicular to the surface of the amorphous samples. As is known, there exists a magnetic anisotropy (attributable mainly to shape anisotropy) in the quenched state of amorphous alloys, when the average direction of spin is (relatively) closer to the ribbon plane ($A_{2.5}/A_{1.6} > 2/3$ and $\theta > 45°$) than to the normal (e.g., [40]).

Our results show a dose dependent decrease of magnetic anisotropy in amorphous materials irradiated with energetic heavy ions.

In rapidly quenched, amorphous ferromagnetic alloys the domen pattern and magnetization processes are governed by topological defects and their stress fields, as shown by Kronmüller [37]. The domen pattern reflects the arrangement of tensile and compressive stresses. The defects formed during the rapid quenching process by a special distribution of free volume were considered as the sources of stresses [36].

Our finding can be associated with the defects induced by irradiation because of the corresponding changes in the orientation of spins depending on the direction of stresses occurring around these defects (see Fig.7). On the other hand, some contribution from spin reorientation around the stress centres formed during the inhomogeneous solidification process as a consequence of mixing of atoms due to irradiation has to be taken into consideration.

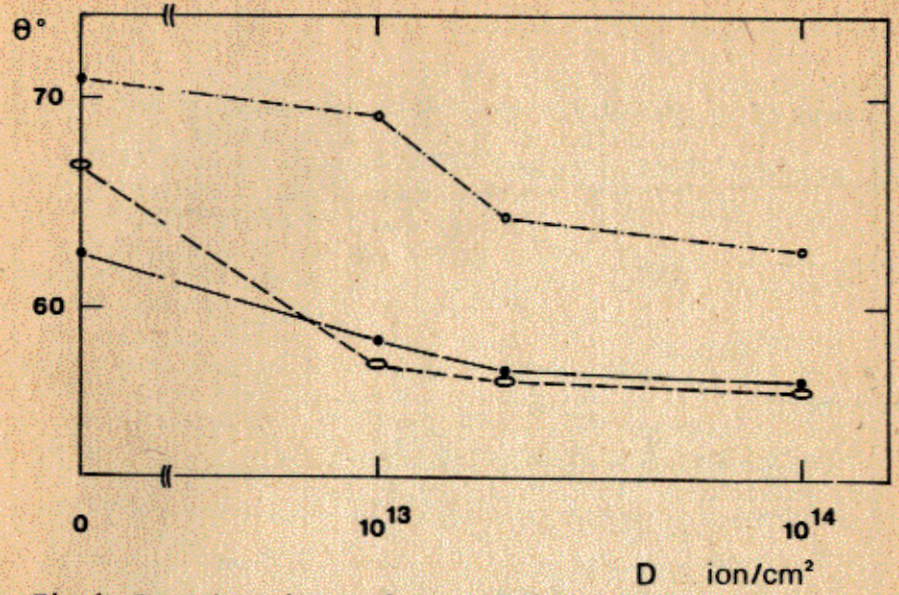

Fig.6. Dose dependence of θ angle (between the γ ray direction and the average direction of magnetic moment) for some Ar-irradiated $Fe_{40}Ni_{40}B_{20-x}Si_x$ amorphous alloys (o x = 0, x = 5, • x = 10).

The results of the density [6], electrical resistivity [26] and profilometry [22] measurements were interpreted as radiation induced deflects in amorphous alloys, and this confirms our conclusion.

The changes of the hyperfine field distribution, as well as of the average hyperfine parameters, can be interpreted as changes in the short-range order, because in these systems the iron hyperfine field is propotional to the iron magnetic moment, which is determined mainly by a number of nearest metalloid neighbours [42,39,43]. The quantitative correspondence of the field with the coordination and geometrical arrangements of atoms in four component Fe-Ni-Si-B metal-metalloid amorphous alloy is not clarified yet, but it is possible to suppose a similar tendency of changes in two component Fe-M systems, for which case an empirical relationship was found [43]. It follows qualitatively that the hyperfine field decreases as the distance between the iron and metalloid atoms decreases, and vice versa. Thus the hyperfine field distribution is determined by the metalloid distribution around the iron atoms and it provides the probability for the presence of an iron atom with a given number of metalloid neighbours. The isomer shift gives similar information with less sensitivity.

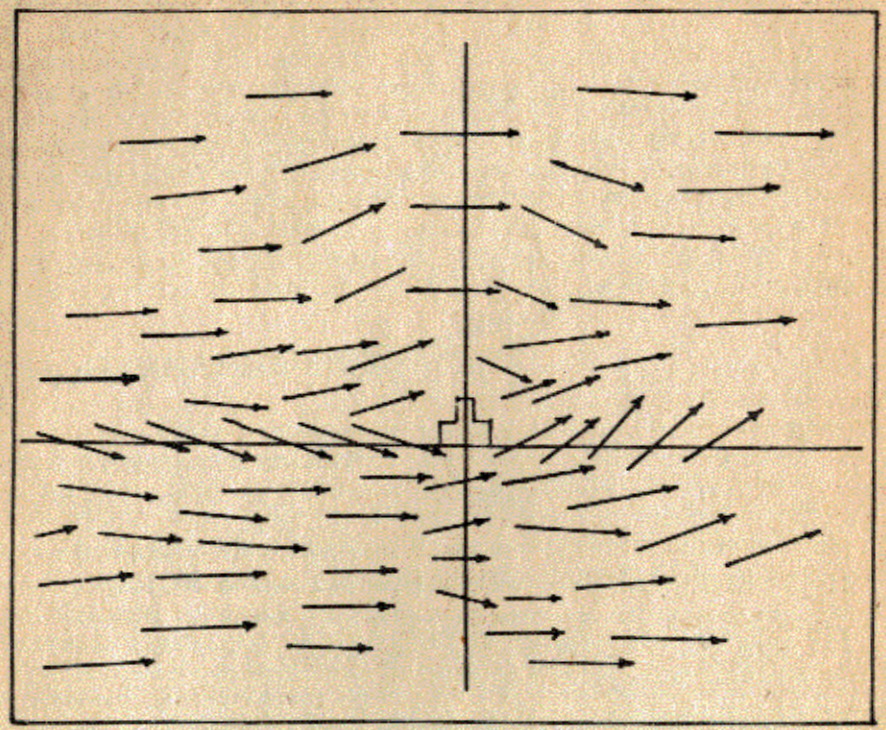

Fig.7. Arrangement of spins around a defect in amorphous alloy.

The geometrical arrangement of metalloids and transition metal neighbours (mainly the geometrical symmtery) is reflected in the quadrupole interaction ΔE_Q which can be expressed in the form [27]

$$\Delta E_Q = k \cdot e \cdot Q \cdot V_{zz} \left(1 + 1/3 \cdot \eta^2\right)^{\frac{1}{2}}, \qquad (2)$$

where V_{zz} is the principal component of diagonalized electric field gradient tensor at the site of the nucleus, Q is the nuclear quadrupole moment, $\eta = V_{xx} - V_{yy}/V_{zz}$, $|V_{zz}| \geq |V_{yy}| \geq |V_{xx}|$, is the asymmetry parameter. In the case of the point charge model approximation, in which the charges of distant atoms, surrounding the Mössbauer atom in non-cubic symmetry, V_{zz} and η can be computed using the formulae [27]

$$V_{zz} = \sum_i q_i \cdot r_i^{-3} \cdot (3 \cdot \cos^2\theta_i - 1), \qquad (3)$$

$$= 1/V_{zz} \sum_i q_i \cdot r_i^{-3}\, 3 \cdot \sin^2\theta_i \cdot \cos^2\phi_i, \qquad (4)$$

where r_i is the charge distance, ϕ_i and θ_i are the polar angles, q_i is the effective charge with respect to Mössbauer atom. Hence it can be understood that the quadrupole splitting can provide information about the homogeneous change of interatomic distances in amorphous alloys in a special case.

The observed broadening of the hyperfine field distribution of the irradiated samples compared with that of nonirradiated ones is attributable to the increasing degree of disorder because it represents iron atoms having a wider variety of arrangements of neighbourhoods in the irradiated alloys, than that of nonirradiated ones.

Moreover it may reflect some decrease of the chemical short-range order existing in our case. Namely Vincze et al. [39] have concluded that the substitution of Ni into Fe-B amorphous increases significantly the degree of ordering because B atoms prefer to be surrounded by Ni atoms. Accordingly they found the hyperfine field distributions of Ni substituted amorphous metals to be narrower compared to those in which Ni is absent.

Our latter conclusion can be confirmed by the observed shift of the maximum of the hyperfine field distribution in the case of irradiated samples. The hyperfine field can, for example, decrease when a metalloid atom being near to Ni (as a consequence of chemical short-range order) comes nearer to Fe atoms due to irradiation. Consequently, the shift of the maximum as well as the decrease of the average magnetic field can be attributed mainly to the decrease of chemical short-range order due to irradiation.

Our conclusion is in agreement with those drawn from the results of investigation of radiation effects using other methods [1, 20, 26].

Indirect evidence for our interpretation is obtained in the case of low temperature relaxation of amorphous alloys (when opposite processes were considered, as in our case) when opposite changes of Mössbauer parameters were found [40].

The changes of the shape of the hyperfine field distribution can be associated with defects being in the form of regions having different mass densities (as was proposed [24, 44]). The right-hand side of the maximum may represent such regions (with increased metal-metalloid distances) having positive free volume, to the left side from the maximum can contribute to such regions (with decreased metal-metalloid distances) having negative free volumes. From the comparison of shape distortions on the left-to-the-right side of the maximum in the hyperfine field distribution of the irradiated sample with the nonirradiated sample, even if we neglect the contribution of changes in the chemical short-range order, we can observe that the right-hand side overcompensates the left one. This means that the

excess free volume introduced by the irradiation exists in the irradiated samples. This is in agreement with other authors's findings [6,26].

Our conclusions drawn from the Mössbauer results of the studies of amorphous samples are confirmed by the changes caused by irradiation in the Mössbauer parameters of Fe-Ni-P amorphous alloys, being in paramagnetic states. The observed quadrupole splitting decrease due to irradiation can be attributed to the decrease of the chemical short-range order as well as to the increase of the average interatomic distances. From the comparison of the paramagnetic spectra of Ni substituted amorphous with those in which the Ni was absent [39] it is found that the quadrupole splitting is higher in Ni substituted alloys as a result of the increased asymmetry due to the ordering. According to this result, our oppositely directed change of quadrupole splitting requires an opposite interpretation, namely the decrease in chemical short-range order.

Beside this, the homogeneous increase of the interatomic distances can also be reflected in the decrease of average quadrupole splitting due to irradiation. By neglecting the contribution of a change in chemical short-range order we can estimate using eq. (2-4) the upper limit of an increase of the average interatomic distance to be 1%. By taking into account the contribution of chemical short-range order changes in the decrease of average quadrupole splitting, we can obtain data on a change of average interatomic distances, which are in good agreement with those of the density measurements of Kramer et al. [6].

5. CONCLUSIONS

The following conclusions can be drawn from the changes of the Mössbauer parameters of the $Fe_{40}Ni_{40}B_{20-x}Si_x$ and $Fe_xNi_{80-x}P_{20}$ amorphous alloys irradiated with ^{40}Ar (E = 225 MeV) and ^{132}Xe (E = 120 MeV) ions, compared to those of nonirradiated ones:

1. The degree of disorder increases.
2. Defects are introduced, the excess free volume and the average interatomic distance increase.
3. The magnetic anisotropy decreases with a change in spin orientation around the radiation-induced defects, as well as the quenched in stress source.
4. The chemical short-range order decreases as a result of remixing of atoms due to irradiation.

ACKNOWLEDGEMENTS

We wish to thank Prof. T.Ruskov, Dr. V.A.Schegolyev, Dr. Gy.Szenes for discussions, Dr. A.Didyk for his help in the irradiation, Dr. S.Nagy, Prof. A.Vertes for control measurements, as well as Prof. G.N.Flerov and Prof. Yu.Ts.Oganessian for providing the opportunity to perform the work.

REFERENCES

1. Lesueur D. Rad. Eff., 1975, 24, p. 101.
2. Nanao S. et al. Proc. 4th Int.Conf. on Rapidly Quenched Metals (Sendai, 1981, 3.6/9/).
3. Moser P. et al. Proc. 4th Int.Conf. on Rapidly Quenched Metals (Sendai, 1981, 3.6/3/).
4. Hautojärvi P., Ili-Kaupilla J. J.Nucl.Methods, 1982, 199, p. 75.
5. Nandedkar R.V., Tyagi A.K., Varatharajan K. Proc. 4th Int. Conf. on Rapidly Quenched Metals (Sendai, 1981, 3.6/2/).
6. Kramer E.A., Cline W.L. Appl.Phys.Lett., 1979, 351, p. 815.
7. Itoh F. et al. Proc. 4th Int.Conf. on Rapidly Quenched Metals (Sendai, 1981, 3.6/4/).
8. Doi K., Ayano H., Masumoto T. Appl.Phys.Lett., 1977, 31, p. 421.
9. Doi K., Ayano H., Kawamura K. J.Noncryst.Sol., 1979, 34, p. 405.
10. Cerling R., Wagner R. Proc. 4th Int.Conf. on Rapidly Quenched Metals (Sendai, 1981, 3.6/5/).
11. Cahn R.W. et al. Proc. 4th Int.Conf. on Rapidly Quenched Metals. Sendai, 1981, p. 789.
12. Clins C.F., Hopper R.W., Johnson W.L. Proc. 4th Int. Conf. on Rapidly Quenche Metals (Sendai, 1981, 3.6/7/).
13. Goldanskii V.I. et al. Proc. Int.Conf. on the Application of the Mössbauer Effect. Nauka, Alma-Ata, 1983, p. 58.
14. Yadawa R.D.S. et al. J.Nucl.Mater., 1980, 92, p. 366.
15. Tyagi A.K., Nandedkar R.V. Proc. 4th Int.Conf. on Rapidly Quenched Metals (Sendai, 1981, 3.6/6/).
16. Paszti F. et al. Phys.Rev., 1983, 28, p. 5688.
17. Lovas I., Paszti F. Phys.Rev., 1983, 28, p. 5692.
18. Nasu S., Fujita F.E. Proc.Int. Conf. on the Application of the Mössbauer Effect.Nauka, Alma-Ata, 1983, p. 504.
19. Van Swijgenhoven H., Stals L.M. Proc. 4th Int.Conf. on Rapidly Quenched Metals (Sendai, 1983, 3.6/8/).
20. Hillatret J. et al. J. de Phys., 1980, 41, C8-854.
21. Azam R. et al. J.Delaplace, J. Nucl.Mater., 1978, 83, p. 298.
22. Rechtin M.D., Vander Sande J., Baldo D.M. Scripta Met., 1978, 12, p. 639.

23. Brimhall J.L., Charlot L.A., Wang R. Scripta Met., 1979, 13, p. 217.
24. Chang B.T., Li J.C.M. Scripta Met., 1977, 11, p. 933.
25. Kuzmann E., Spirov I.N. Proc.Int.Conf. on the Application of of the Mössbauer Effect. Nauka, Alma-Ata, 1983, p. 438.
26. Audoard A., Jousset J.C., Dural J. J. de Phys., 1980, 41, C8-835.
27. Gonser U. Mössbauer Spectroscopy (ed. by U.Gonser), Springer, Heidelberg, N.Y., 1975.
28. Gonser U. et al. J. de Phys., 1979, 40, C2-126.
29. Fujita F.E. J. de Phys., 1979, 40, p. 120.
30. Vincze I. et al. Proc. Conf. on Metallic Glasses, Budapest, 1980 , p. 361.
31. Klein H.P. et al. J.Nucl.Meth., 1982, 199, p. 159.
32. Tomov T.T. et al. Proc. Int.Conf. on the Application of the Mössbauer Effect. Nauka, Alma-Ata, 1983, p. 421.
33. Kuzmann E., Oshima R., Fujita F.E. Proc. Int.Conf. on the Application of the Mössbauer Effect. Jaipur, 1981, p. 553.
34. Seagusa N., Morrish A.H. Phys.Rev.B, 1982, B26, p. 10.
35. Bardos G., Fedyanin V.K., Gavrilenko G.M. JINR, E17-83-303, Dubna, 1983.
36. Kronmüller H., Fernengel F. phys.stat.sol., 1981, 64, p. 593.
37. Kronmüller H. J. de Phys., 1980, 41, C8-618.
38. Chien C.L. Sol.State Comm., 1977, 24, p. 231.
39. Schaafsma A.S. et al. J. de Phys., 1980, 41, C8-246.
40. Kemeny T. et al. J. de Phys., 1980, 41, C8-879.
41. Gonser U. J. de Phys., 1980, 41, C1-51.
42. Panissod P., Durand J., Budnick J.I. Nucl.Instr.Meth., 1982, 199, p. 99.
43. Lines M.E. Sol.State Comm., 1980, 36, p. 457.
44. Egami T. et al. J. de Phys., 1980, 41, C8-273.

Received by Publishing Department
on May 18, 1984.

SUBJECT CATEGORIES OF THE JINR PUBLICATIONS

Index	Subject
1.	High energy experimental physics
2.	High energy theoretical physics
3.	Low energy experimental physics
4.	Low energy theoretical physics
5.	Mathematics
6.	Nuclear spectroscopy and radiochemistry
7.	Heavy ion physics
8.	Cryogenics
9.	Accelerators
10.	Automatization of data processing
11.	Computing mathematics and technique
12.	Chemistry
13.	Experimental techniques and methods
14.	Solid state physics. Liquids
15.	Experimental physics of nuclear reactions at low energies
16.	Health physics. Shieldings
17.	Theory of condenced matter
18.	Applied researches
19.	Biophysics

Кузьман Е., Спиров И.Н. E14-84-339

Мессбауэровское исследование аморфных сплавов, облученных тяжелыми ионами высокой энергии

Методом мессбауэровской спектроскопии были исследованы радиационные повреждения в аморфных сплавах, облученных ионами ^{40}Ar / E = 225 МэВ/ и ^{132}Xe / E =120 МэВ/ при комнатной температуре. Наблюдалось зависящее от дозы уменьшение второй и пятой линии в мессбауэровских спектрах, а также уменьшение среднего магнитного поля. Эти изменения анализировалась с использованием распределений магнитных полей, полученных из мессбауэровских спектров. Результаты интерпретируются в свете представлений дефектообразования и структурных изменений ближнего порядка облученных аморфных сплавов.

Работа выполнена в Лаборатории ядерных реакций ОИЯИ.

Препринт Объединенного института ядерных исследований. Дубна 1984

Kuzmann E., Spirov I.N. E14-84-339

Mössbauer Study of Amorphous Alloys Irradiated with Energetic Heavy Ions

The Mössbauer spectroscopy was applied to study radiation damages in amorphous alloys irradiated with ^{40}Ar (E=225 MeV) or ^{132}Xe (E = 120 MeV) ions at room temperature. In the magnetically splitted Mössbauer spectra the dose-dependent decreases of the intensity of the 2nd and 5th lines as well as of the average hyperfine magnetic field were observed. The changes were also analysed using the hyperfine field distribution obtained from the spectra. The results are interpreted in terms of defect creation and structural changes of short-range order of irradiated amorphous alloys.

The investigation has been performed at the Laboratory of Nuclear Physics, JINR

Preprint of the Joint Institute for Nuclear Research. Dubna 1984